Giant Splitting of the Hydrogen Rotational Eigenenergies in the C_2 Filled Ice

Simone Di Cataldo,[1,2,*,§] Maria Rescigno,[1,3,*,†] Lorenzo Monacelli,[1] Umbertoluca Ranieri,[4] Richard Gaal,[3] Stefan Klotz,[5] Jacques Ollivier,[6] Michael Marek Koza,[6] Cristiano De Michele,[1] and Livia Eleonora Bove[1,3,5,‡]

[1]*Dipartimento di Fisica, Sapienza Università di Roma, Piazzale Aldo Moro 5, 00187 Roma, Italy*

[2]*Institüt für Festkörperphysik, TU Wien, Wiedner Hauptstraße 8-10, Vienna 1050, Austria*

[3]*Laboratory of Quantum Magnetism, Institute of Physics, École Polytechnique Fédéerale de Lausanne, CH-1015 Lausanne, Switzerland*

[4]*Centre for Science at Extreme Conditions and School of Physics and Astronomy, University of Edinburgh, EH9 3FD Edinburgh, United Kingdom*

[5]*Sorbonne Université, UMR CNRS 7590, Institut de Minéralogie, de Physique des Matériaux et de Cosmochimie (IMPMC), 5 Place Jussieu, 75005 Paris, France*

[6]*Institut Laue-Langevin, 71 Avenue des Martyrs, Cedex 9, Grenoble, France*

(Received 23 May 2024; accepted 31 October 2024; published 6 December 2024)

Hydrogen hydrates exhibit a rich phase diagram influenced by both pressure and temperature, with the so-called C_2 phase emerging prominently above 2.5 GPa. In this phase, hydrogen molecules are densely packed within a cubic icelike lattice and the interaction with the surrounding water molecules profoundly affects their quantum rotational dynamics. Herein, we delve into this intricate interplay by directly solving the Schrödinger's equation for a quantum H_2 rotor in the C_2 crystal field at finite temperature, generated through density functional theory. Our calculations reveal a giant energy splitting relative to the magnetic quantum number of ± 3.2 meV for $l = 1$. Employing inelastic neutron scattering, we experimentally measure the energy levels of H_2 within the C_2 phase at 6.0 and 3.4 GPa and low temperatures, finding good agreement with our theoretical predictions. These findings underscore the pivotal role of hydrogen-water interactions in dictating the rotational behavior of the hydrogen molecules within the C_2 phase and indicate heightened van der Waals interactions compared to other hydrogen hydrates.

DOI: 10.1103/PhysRevLett.133.236101

The phase behavior of hydrogen hydrates represents a captivating realm of inquiry at the intersection of physics and quantum chemistry, offering insights into the complex interplay of molecular interactions under extreme conditions and quantum motions under extreme confinements. At pressures (P) above 0.1 GPa and below ~0.5 GPa, mixtures of water and hydrogen molecules crystallize in a non-stoichiometric clathrate compound, which is characterized by polyhedral cavities formed by hydrogen-bonded water molecules encaging a variable amount of nonbonded H_2 molecules [1–5]. The dynamics of the (freely rotating) hydrogen molecules within the cages stabilizes the highly porous ice structure [6]. At low temperatures (T), the quantum motion of the "encaged" guest H_2 molecules has been characterized by means of inelastic neutron scattering and Raman spectroscopy experiments, mostly on samples recovered to ambient pressure [7–10], and reveals to be similar to the one observed for H_2 trapped in other nanocavities [11–18]. The anisotropy in the hydrogen-water interaction potential has been shown to be effective in splitting the quantized translational and rotational energy levels; however, such splittings are rather small, indicating a weak guest-host interaction. Bačić and coworkers [19] led the way in developing the theoretical framework for describing this cage potential, resulting in a more precise assessment of the energy levels that define the quantum dynamics of H_2. These computational studies shed light on a crucial aspect of dynamics: the interaction between translational and rotational angular momentum. We model the H_2-cage interaction using a 5D-cage potential, which describes both the H_2 molecule orientation and the coordinates of its center of mass [17,19–21]. The quantum dynamics of the H_2 molecule confined in a clathrate hydrate structure was also studied as a function of pressure up to 0.5 GPa [22], showing only a small impact on the energy levels and splittings despite the varying water-hydrogen distances with pressure.

At pressures above ~0.5 GPa, hydrogen hydrates adopt so-called "filled ice" phases, in which the water sublattice is structurally similar to ice [2,23–32] and hydrogen molecules occupy defined positions inside the icelike channels. In the filled ice C_1 phase, which is constituted by an ice-II-like host frame and has a 1:6 hydrogen to water

*These authors contributed equally to this letter.
†Contact author: maria.rescigno@uniroma1.it
‡Contact author: livia.bove@upmc.fr
§Contact author: simone.dicataldo@uniroma1.it

molecular ratio [25–27], the first rotational energy level of the confined H_2 was found (by inelastic neutron scattering at high pressure and low temperature) to be only marginally different from that of a free H_2 rotor [22]. Similar results [33] were observed for the quantum dynamics of H_2 confined in the C_0 structure of hydrogen hydrate, where the host water lattice is not based on any stable ice phase [23,24,34]. Among the diverse filled ice phases, the C_2 phase (stable above ~2.5 GPa) stands out for its distinctive characteristics arising from the interplay between hydrogen and water molecules, which form two identical and interpenetrated ice-I *c*-like (or diamondlike) sublattices with a 1:1 hydrogen to water molecular ratio. As a result, hydrogen molecules are very densely packed in this structure and the hydrogen-water distances are very short [27–30,35]. One of the remarkable features of the C_2 phase is indeed the profound influence of the surrounding water molecules on the quantum dynamics of the encapsulated hydrogen molecules. Unlike in other phases, in the C_2 phase, the crystal field imposed by the water molecules is expected to strongly affect the quantum rotational dynamics of the H_2 molecules. To our knowledge, the quantum mechanical behavior of molecular hydrogen within the C_2 lattice has not been explored yet. Above ~40 GPa, the C_2 phase transforms into the C_3 phase upon laser heating [36,37], which has an identical cubic water sublattice but is even richer in H_2 (2:1 molecular ratio), resulting in significant unit cell expansion and consequent larger hydrogen-water distances. Therefore, the C_2 phase represents the most extreme case of confinement for hydrogen molecules in a water frame and thus provides an ideal benchmark to study the quantum motion of hydrogen in strong confinement.

In this work, we employed state-of-the-art computational and experimental techniques to fully characterize the rotational quantum dynamics of the H_2 molecules in the C_2 phase at low temperatures. In particular, we solve the 3D Schrödinger's equation for a hydrogen molecule (rotational and vibrational degrees of freedom) in the effective crystal field of the C_2 phase: the H_2 effective potential at finite temperature computed within *ab initio* molecular dynamics accounting for van der Waals corrections to the exchange-correlation functional. Our calculations reveal that the H_2O-H_2 interaction is such to induce a giant splitting of ± 3.2 meV in the $l = 1$ rotational eigenenergies. To validate our theoretical predictions and further probe the quantum rotational dynamics of H_2 within the C_2 phase, we employ inelastic neutron scattering (INS), a powerful experimental technique capable of providing detailed insights into the energy levels of hydrogen molecules. Through pioneering INS experimental measurements conducted at 6 GPa and low temperature ($4\ \mathrm{K} < T < 85\ \mathrm{K}$), we corroborate our theoretical findings, thereby affirming the accuracy of our predictions regarding the quantum rotational dynamics of H_2 within the C_2 phase.

Our results not only deepen the understanding of the fundamental physics governing hydrogen hydrates and shed light on the hydrogen-water interaction in dense systems, but also carry broader implications for molecular hydrogen under extreme conditions. Furthermore, the observed heightened interactions in the C_2 phase underscore the significance of hydrogen hydrates in diverse fields ranging from materials science to astrochemistry.

The H_2 molecule is the textbook example of a quantum rigid rotor, with rotational peaks equally spaced and separated by $2B = \hbar^2/I$, where I is the moment of inertia $\mu R^2 = (mR^2/2)$, with μ the reduced mass, m the mass of H_2, and R the H-H distance. The Schrödinger's equation extends to the case of an external potential V_{ext} (Cartesian coordinates, atomic units),

$$\left(-\frac{\nabla^2}{2\mu} + V_{\mathrm{ext}}(\vec{r})\right)\psi_n(\vec{r}) = \epsilon_n \psi_n(\vec{r}). \tag{1}$$

For a H_2 molecule in the C_2 crystal, the van der Waals interactions between H_2 and the water sublattice can be modeled precisely with such an effective potential V_{ext}. We neglect quantum fluctuations in the host lattice. Within this approximation, at 0 K, V_{ext} is the total energy of the crystal at various hydrogen orientations. Temperature can also be accounted for by replacing V_{ext} with the free energy landscape averaged over different snapshots from molecular dynamics at the chosen temperature [see Supplemental Material (SM) for further details [38]]. The calculations were performed using the density functional theory relaxed structure of C_2 having the correct experimental volume (see Table S2 in SM [38] for full structural details). The result is the effective potential shown in Fig. 1, split into its radial ($|r|$) and angular (θ, ϕ) components. The radial component is very well fitted by a Morse potential, while the angular part is characterized by a complex landscape well reproduced by a combination of sines and cosines (see SM [38]). We note that these calculations neglect the effect of H_2-H_2 interaction, either directly or mediated by the water sublattice. An estimate of the effect of a direct interaction is shown in SM [38].

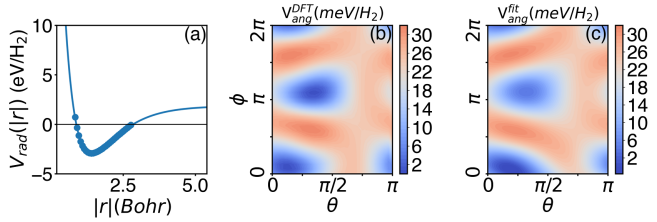

FIG. 1. (a): Radial part of the potential (V_{rad}). Density functional theory calculated data points are shown as blue circles and the fit with the Morse potential is shown as a blue line. The energy zero is taken as the last calculated point. Panels (b) and (c) show the calculated and fitted angular part of the potential [$V_{\mathrm{ang}}(\theta, \phi)$], respectively, at a temperature $T = 10$ K. See Supplemental Material [38] for further details.

The Schödinger's equation (1) with the calculated V_{ext} was solved numerically using the Lanczos algorithm in shift-invert mode to obtain the lowest-energy eigenvalues and eigenfunctions. In Fig. 2(a), we show the energy states compared to the free rotor. We remark that H_2 molecules being constituted of two identical fermionic hydrogens form two spin isomers, namely *para*-hydrogen (p-H_2) with nuclear spin number $I = 0$ and *ortho*-hydrogen (o-H_2) with nuclear spin number $I = 1$. Because of total wave function symmetry constraints, p-H_2 can only be associated with even rotational quantum number states ($l = 0, 2, 4\ldots$) and o-H_2 with odd states ($l = 1, 3\ldots$). To benchmark the solver, Fig. 2(a) shows that our method is consistent with the analytic result in the absence of V_{ext}. When the host lattice is accounted for, the magnetic quantum number m degeneracy is broken with a splitting of ± 3.2 meV for $l = 1$.

In Fig. 2(b), we show the wave functions corresponding to the ground state and the first three excited levels. The host crystal field breaks the rotational symmetry of the molecule, and both l and m are no longer good quantum numbers. However, the low-energy states still keep a dominant l value that can be used to group states, while the m states with a similar l are mixed to form oriented orbitals that we number with an index λ [see Fig. 2(b) and Sec. S2B of SM [38] for more details). It is easier to interpret the wave functions in comparison with the spherical harmonics, i.e., the result for the unperturbed rotor (shown in Fig. S7): the ground-state wave function is shaped like a hollow hemisphere, i.e., localized around $|\vec{r}| \sim R$. Unlike the unperturbed rotor (where the wave function is a perfect sphere), this wave function exhibits a broken angular symmetry in the direction of the minimum of the potential. The first excited state wave function is oriented roughly in the same direction as the ground state, while the other two point in orthogonal directions, like the p_x, p_y, and p_z angular orbitals of the hydrogen atom.

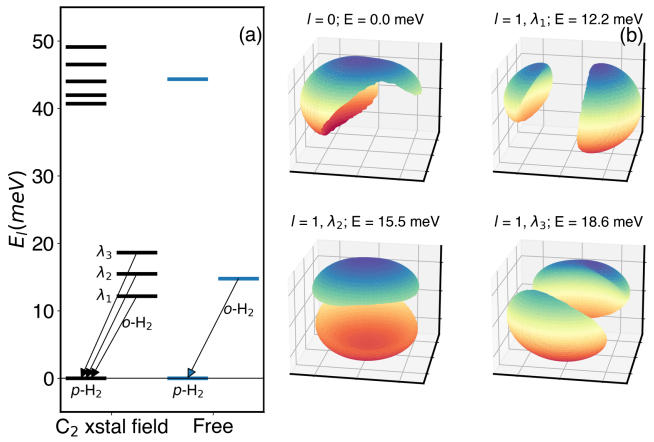

FIG. 2. (a) Calculated energy levels for the quantum rotations of the H_2 molecule in the C_2 phase (black) and for the free rotor (blue). The eigenenergies are divided into *even-l* (p-H_2) and *odd-l* ones (o-H_2). Arrows indicate the transition from ortho-H_2 ($l = 1$) to para-H_2 ($l = 0$). (b) Isosurfaces showing the eigenfunctions of the ground state and the first three excited states of the H_2 molecule in the C_2 crystal field (isolevel: $7e - 5$), the color indicates the z axis and is used as a visual aid. The total angular momentum l, index λ, and eigenenergies are given.

Transitions between quantum rotational levels can be directly measured with inelastic neutron scattering. In particular, as transitions between the ground state ($l = 0$) and the first excited state ($l = 1$) involve changes in the nuclear spin, INS is the only experimental technique able to directly measure the fundamental rotational transition of molecular hydrogen. In addition, thanks to the long-lived metastable nature of the ortho state [47], the ortho-para transition can be measured in the neutron energy gain side of the dynamical structure factor even at low temperature (see paragraph S5 E in [38]) [16]. Previous studies focusing on hydrogen molecules trapped in molecular cages of different sizes showed that rotational transitions can combine with low-energy rattling modes [9,22], leading to many possible combinations. In the C_2 hydrate, however, rattling modes are out of the probed energy window due to the short average H_2-H_2O distances, leading to a much simpler INS spectrum, as shown in Fig. 3(a).

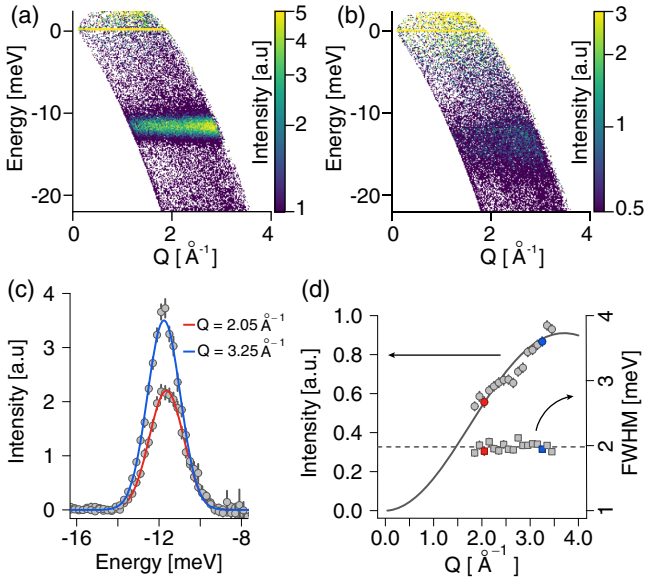

FIG. 3. INS experimental data and Q analysis. (a) $S(Q, \omega)$ after data reduction at 4.4 K and 6 GPa. A strong inelastic feature is observed at about -11.7 meV. (b) $S(Q, \omega)$ after data reduction at 85 K and 6 GPa. The strong inelastic feature is broadened and the intensity decreases at high temperature as the higher energy levels are populated. (c) Q binned spectra and their Gaussian fits for $Q = 2.05$ Å^{-1} (red line) and $Q = 3.25$ Å^{-1} (blue line). (d) FWHM of the Gaussian fits to the Q-sliced INS spectra as a function of Q (squares, right axis) and integrated intensity of the Gaussian fits to the Q-sliced INS spectra as a function of Q (circles, right axis) and its best fit (see Supplemental Material [38] for further details).

Two INS experiments were performed on the IN5 time-of-flight spectrometer at ILL in Grenoble, France (raw data available at [48,49]). The H_2:D_2O sample was loaded cryogenically in a Paris-Edinburgh press (see SM [38] for further details on the sample preparation and environment). In the first experiment, the sample was compressed to 6.0 GPa (see Fig. S10) and cooled down to 4.4 K; in the second, it was cooled to 9 K. In both experiments the incoherent dynamical structure factor $S(Q,\omega)$ was measured using an incident wavelength of 4.8 Å, thus mainly measuring in the neutron energy gain side. The results from the first run are shown in Fig. 3(a), while those from the second run are shown in SM (Fig. S12) [38] and in Fig. 3(b).

In both experiments, we observed the first ortho-para ($l=1$, λ_1 to $l=0$) transition of the hydrogen molecules confined in the C_2 phase to have an energy of 11.7 meV, i.e., about 3 meV lower compared to the ortho-para transition of free hydrogen (14.6 meV). The rotational nature of the excitation peak observed in the $S(Q,\omega)$ is confirmed from the exchanged wave vector Q analysis of both peak width and intensity. After Q slicing the $S(Q,\omega)$, the spectra [Fig. 3(c)] can be fitted with Gaussian functions, whose FWHM are found to be constant with Q [Fig. 3(d)] and whose intensities are well described by a squared first-order spherical Bessel function [Fig. 3(d)]. Both of these trends are indicative of a rotational nature for the excitation. As the temperature was increased up to 85 K, we observed a progressive population of the higher energy levels ($l=1$, λ_2, and $l=1$, λ_3) and the consequent associated transition to the ground state (see Fig. S11 for a schematic representation of the observed transitions). In Fig. 4(a) we show the Q-integrated $S(Q,\omega)$ for $T=8$, 33, and 85 K, together with their best fits. The three peaks (different shades of blue) that appear at 85 K correspond to the transitions from λ_1, λ_2, and λ_3 to the ground state while the sharp peak (gray area) originates from pure hydrogen in the sample. The occupation of the levels is in good agreement with the Boltzmann distribution and the splitting of the ortho-H_2 level is of ± 2.2 meV, 30% smaller than in our calculations [yellow diamonds in Fig. 4(b)]. Examples of INS spectra [obtained by integrating the $S(Q,\omega)$ over the whole measured Q range], compared with their best fits, and fit results are shown in Fig. 4. The Q analysis of the data shows a consistent behavior also at the highest investigated temperatures (see Fig. S16). The sample was then decompressed to 3.4 GPa at 85 K and measured at 5 K and 33 K [squares in Fig. 4(b), spectra are reported in S17], where we observed a 7.5% reduction of the energy splitting. In addition, we observed that the rotational transitions show an intrinsic broadening much larger than our experimental resolution (0.8 meV), which can be attributed to structural defects formed upon compression (see Fig. S18).

Overall, we find the calculated and experimental results for the energy levels in good agreement in terms of both the absolute values and the energy splitting [see Fig. 4(b)]. The largest discrepancy is for the high-energy mode. The discrepancy decreases with increasing temperature. This is expected as the temperature dependency of our model comes from the thermal activation of the phonons of the host water frame, altering the effective potential on the H_2 molecule. The zero-point motion of the ice skeleton, which becomes significant at very low temperatures, is neglected by our classical molecular dynamics sampling. Indeed, as temperature increases, the classical sampling of the ice phonons improves as the agreement between simulations and experimental data.

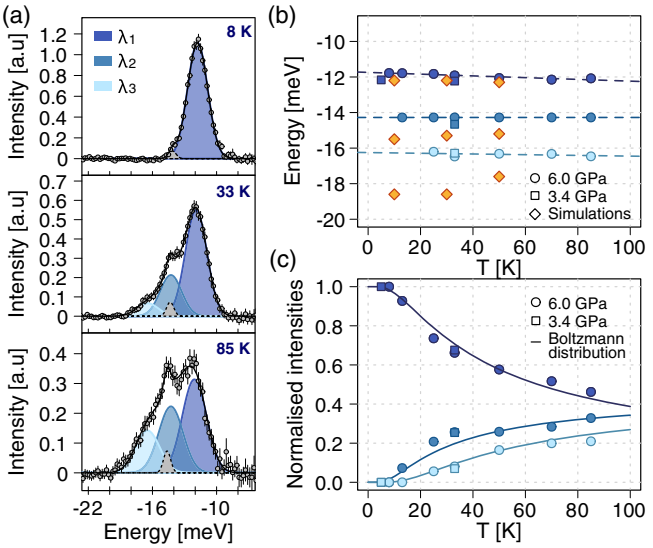

FIG. 4. Temperature dependence of the INS experimental results. (a) INS spectra at 6 GPa and 8 K, 33 K, 85 K, compared to their best fits (blue areas). The gray shaded area is the peak from the pure solid hydrogen in the sample. (b) Energies of the three rotational peaks at 6.0 and 3.4 GPa (blue circles and squares respectively) as a function of temperature compared with numerical results (yellow diamonds). (c) Normalized intensities of the three peaks at 6.0 and 3.4 GPa (blue circles and squares respectively) compared to the statistical weights of the initial states calculated using the Boltzmann distribution. Plots with error bars are reported in Fig. S14 in Supplemental Material [38]. The different blue shades are consistently associated to the transitions from the λ_1, λ_2, λ_3 levels to the ground state as shown in the legend.

In summary, we studied the quantum dynamics of the H_2 molecule in the C_2 filled ice phase at high pressure and low temperature. The overall good agreement between our calculations and the experimental results offers a simple interpretation of the data. In the C_2 phase, the H_2 and water interact quite strongly, leading to a strong angular anisotropy in the effective crystalline potential felt by the hydrogen molecule. This crystal field lifts the angular degeneracy of the rotational triplet state ($l=1$) with respect to the magnetic quantum number m, resulting in an energy splitting of ± 3.2 meV in our calculations and

±2.2 meV experimentally. To the best of our knowledge, such a large splitting in the energy levels of a quantum rotor in a water-based clathrate is unprecedented. As the C_2 hydrate is stable (or metastable) over a wide pressure range spanning from nearly ambient pressure (at low temperature) [2,35] to pressures above 80 GPa at least [37], it represents an ideal playground to further explore low-energy physics of quantum rotors in the future.

Acknowledgments—We acknowledge the Institut Laue-Langevin (ILL) for providing beam time on IN5 and the assistance from Claude Payre with the high-pressure setup. We thank Leon Andriambariarijaona and Alasdair Nicholls for their help during the experiments on IN5, and Thomas C. Hansen for technical assistance during the experiment on D20. We thank Lorenzo Ulivi, Leonardo del Rosso, and Milva Celli for providing the sample. S. D. C. acknowledges computational resources from CINECA, proj. IsC90-HTS-TECH and IsC99-ACME-C, the Vienna Scientific Cluster, proj. 71754 "TEST". L. E. B. acknowledges the financial support by the European Union—NextGenerationEU (PRIN N. F2022NRBLPT), the ANR-23-CE30-0034 EXOTIC-ICE, and the Swiss National Fund (FNS) under Grant No. 212889.

[1] W. L. Mao, H. kwang Mao, A. F. Goncharov, V. V. Struzhkin, Q. Guo, J. Hu, J. Shu, R. J. Hemley, M. Somayazulu, and Y. Zhao, Hydrogen clusters in clathrate hydrate, Science **297**, 2247 (2002).

[2] W. L. Mao and H. k. Mao, Hydrogen storage in molecular compounds, Proc. Natl. Acad. Sci. U.S.A. **101**, 708 (2004).

[3] K. A. Lokshin, Y. Zhao, D. He, W. L. Mao, H. k. Mao, R. J. Hemley, M. V. Lobanov, and M. Greenblatt, Structure and dynamics of hydrogen molecules in the novel clathrate hydrate by high pressure neutron diffraction, Phys. Rev. Lett. **93**, 125503 (2004).

[4] T. A. Strobel, M. Somayazulu, and R. J. Hemley, Phase behavior of $H_2 + H_2O$ at high pressures and low temperatures, J. Phys. Chem. C **115**, 4898 (2011).

[5] E. F. Bazarkina, I.-M. Chou, A. F. Goncharov, and N. N. Akinfiev, The behavior of H_2 in aqueous fluids under high temperature and pressure, Elements **16**, 33 (2020).

[6] S. Patchkovskii and J. S. Tse, Thermodynamic stability of hydrogen clathrates, Proc. Natl. Acad. Sci. U.S.A. **100**, 14645 (2003).

[7] A. Giannasi, M. Celli, L. Ulivi, and M. Zoppi, Low temperature Raman spectra of hydrogen in simple and binary clathrate hydrates, J. Chem. Phys. **129**, 084705 (2008).

[8] L. Ulivi, M. Celli, A. Giannasi, A. J. Ramirez-Cuesta, D. J. Bull, and M. Zoppi, Quantum rattling of molecular hydrogen in clathrate hydrate nanocavities, Phys. Rev. B **76**, 161401(R) (2007).

[9] D. Colognesi, M. Celli, L. Ulivi, M. Xu, and Z. Bacič, Neutron scattering measurements and computation of the quantum dynamics of hydrogen molecules trapped in the small and large cages of clathrate hydrates, J. Phys. Chem. A **117**, 7314 (2013).

[10] U. Ranieri, L. del Rosso, L. Bove, M. Celli, D. Colognesi, R. Gaal, T. C. Hansen, M. M. Koza, and L. Ulivi, Large-cage occupation and quantum dynamics of hydrogen molecules in sII clathrate hydrates, J. Chem. Phys. **160**, 164706 (2024).

[11] D. G. Narehood, M. K. Kostov, P. C. Eklund, M. W. Cole, and P. E. Sokol, Deep inelastic neutron scattering of H_2 in single-walled carbon nanotubes, Phys. Rev. B **65**, 233401 (2002).

[12] M. Mondelo-Martell and F. Huarte-Larrañaga, 5D quantum dynamics of the H_2@SWNT system: Quantitative study of the rotational-translational coupling, J. Chem. Phys. **142**, 084304 (2015).

[13] S. A. FitzGerald, J. Hopkins, B. Burkholder, M. Friedman, and J. L. C. Rowsell, Quantum dynamics of adsorbed normal-and para-H_2, HD, and D_2 in the microporous framework MOF-74 analyzed using infrared spectroscopy, Phys. Rev. B **81**, 104305 (2010).

[14] T. A. Strobel, A. J. Ramirez-Cuesta, L. L. Daemen, V. S. Bhadram, T. A. Jenkins, C. M. Brown, and Y. Cheng, Quantum dynamics of H_2 trapped within organic clathrate cages, Phys. Rev. Lett. **120**, 120402 (2018).

[15] A. J. Horsewill, K. S. Panesar, S. Rols, M. R. Johnson, Y. Murata, K. Komatsu, S. Mamone, A. Danquigny, F. Cuda, S. Maltsev, M. C. Grossel, M. Carravetta, and M. H. Levitt, Quantum translator-rotator: Inelastic neutron scattering of dihydrogen molecules trapped inside anisotropic fullerene cages, Phys. Rev. Lett. **102**, 013001 (2009).

[16] A. Horsewill, K. Panesar, S. Rols, J. Ollivier, M. Johnson, M. Carravetta, S. Mamone, M. Levitt, Y. Murata, K. Komatsu *et al.*, Inelastic neutron scattering investigations of the quantum molecular dynamics of a H_2 molecule entrapped inside a fullerene cage, Phys. Rev. B **85**, 205440 (2012).

[17] M. Xu, M. Jiménez-Ruiz, M. R. Johnson, S. Rols, S. Ye, M. Carravetta, M. S. Denning, X. Lei, Z. Bačić, and A. J. Horsewill, Confirming a predicted selection rule in inelastic neutron scattering spectroscopy: The quantum translator-rotator H_2 entrapped inside C_{60}, Phys. Rev. Lett. **113**, 123001 (2014).

[18] M. Peña-Alvarez, V. Afonina, P. Dalladay-Simpson, X.-D. Liu, R. T. Howie, P. I. Cooke, I. B. Magdau, G. J. Ackland, and E. Gregoryanz, Quantitative rotational to librational transition in dense H_2 and D_2, J. Phys. Chem. Lett. **11**, 6626 (2020).

[19] M. Xu, F. Sebastianelli, and Z. Bačić, Quantum dynamics of H_2, D_2, and HD in the small dodecahedral cage of clathrate hydrate: Evaluating H_2–water nanocage interaction potentials by comparison of theory with inelastic neutron scattering experiments, J. Chem. Phys. **128**, 244715 (2008).

[20] M. Xu, F. Sebastianelli, Z. Bačić, R. Lawler, and N. J. Turro, H_2, HD, and D_2 inside C60: Coupled translation-rotation eigenstates of the endohedral molecules from quantum five-dimensional calculations, J. Chem. Phys. **129**, 064313 (2008).

[21] F. Sebastianelli, M. Xu, Z. Bačić, R. Lawler, and N. J. Turro, Hydrogen molecules inside fullerene C_{70}: Quantum dynamics, energetics, maximum occupancy, and comparison with C_{60}, J. Am. Chem. Soc. **132**, 9826 (2010).

[22] U. Ranieri, M. M. Koza, W. F. Kuhs, R. Gaal, S. Klotz, A. Falenty, D. Wallacher, J. Ollivier, P. Gillet, and L. E. Bove, Quantum dynamics of H_2 and D_2 confined in hydrate structures as a function of pressure and temperature, J. Phys. Chem. C **123**, 1888 (2019).

[23] D. M. Amos, M.-E. Donnelly, P. Teeratchanan, C. L. Bull, A. Falenty, W. F. Kuhs, A. Hermann, and J. S. Loveday, A chiral gas hydrate structure common to the carbon dioxide water and hydrogen water systems, J. Phys. Chem. Lett. **8**, 4295 (2017).

[24] L. del Rosso, M. Celli, and L. Ulivi, New porous water ice metastable at atmospheric pressure obtained by emptying a hydrogen-filled ice, Nat. Commun. **7**, 13394 (2016).

[25] Y. Wang, K. Glazyrin, V. Roizen, A. R. Oganov, I. Chernyshov, X. Zhang, E. Greenberg, V. B. Prakapenka, X. Yang, S. q. Jiang, and A. F. Goncharov, Novel hydrogen clathrate hydrate, Phys. Rev. Lett. **125**, 255702 (2020).

[26] P. H. B. B. Carvalho, A. Mace, I. M. Nangoi, A. A. L. ao, C. A. Tulk, J. J. Molaison, O. Andersson, A. P. Lyubartsev, and U. Häussermann, Exploring high-pressure transformations in low-Z (H_2, Ne) hydrates at low temperatures, Crystals **12**, 9 (2022).

[27] W. L. Vos, L. W. Finger, R. J. Hemley, and H. kwang Mao, Novel H_2-H_2O clathrates at high pressures, Phys. Rev. Lett. **71**, 3150 (1993).

[28] W. L. Vos, L. W. Finger, R. J. Hemley, and H. kwang Mao, Pressure dependence of hydrogen bonding in a novel H_2O-H_2 clathrate, Chem. Phys. Lett. **257**, 524 (1996).

[29] S.-I. Machida, H. Hirai, and T. Kawamura, Structural changes of filled ice Ic structure for hydrogen hydrate under high pressure, J. Chem. Phys. **129**, 224505 (2008).

[30] H. Hirai, S. Kagawa, T. Tanaka, T. Matsuoka, T. Yagi, Y. Ohishi, S. Nakano, Y. Yamamoto, and T. Irifune, Structural changes of filled ice Ic hydrogen hydrate under low temperatures and high pressures from 5 to 50 GPa, J. Chem. Phys. **137**, 074505 (2012).

[31] L. E. Bove and U. Ranieri, Salt- and gas-filled ices under planetary conditions, Phil. Trans. R. Soc. A **377**, 20180262 (2019).

[32] M. A. Kuzovnikov and M. Tkacz, *T*–*P*–*X* phase diagram of the water–hydrogen system at pressures up to 10 kbar, J. Phys. Chem. C **123**, 3696 (2019).

[33] L. del Rosso, M. Celli, D. Colognesi, S. Rudić, N. J. English, C. J. Burnham, and L. Ulivi, Dynamics of hydrogen guests in ice XVII nanopores, Phys. Rev. Mater. **1**, 065602 (2017).

[34] T. A. Strobel, M. Somayazulu, S. V. Sinogeikin, P. Dera, and R. J. Hemley, Hydrogen-stuffed, quartz-like water ice, J. Am. Chem. Soc. **138**, 13786 (2016).

[35] K. Komatsu, S. Machida, F. Noritake, T. Hattori, A. Sano-Furukawa, R. Yamane, K. Yamashita, and H. Kagi, Ice Ic without stacking disorder by evacuating hydrogen from hydrogen hydrate, Nat. Commun. **11**, 464 (2020).

[36] G.-R. Qian, A. O. Lyakhov, Q. Zhu, A. R. Oganov, and X. Dong, Novel hydrogen hydrate structures under pressure, Sci. Rep. **4** (2014).

[37] U. Ranieri, S. Di Cataldo, M. Rescigno, L. Monacelli, R. Gaal, M. Santoro, L. Andriambariarijaona, P. Parisiades, C. De Michele, and L. E. Bove, Observation of the most H_2-dense filled ice under high pressure, Proc. Natl. Acad. Sci. U.S.A. **120**, e2312665120 (2023).

[38] See Supplemental Material at http://link.aps.org/supplemental/10.1103/PhysRevLett.133.236101 for details of density functional theory calculations, on the solution of the Schrödinger's equation, as well as experimental details. The Supplemental Material includes Refs. [10,37,39–46].

[39] G. Kresse and J. Furthmüller, Efficient iterative schemes for *ab initio* total-energy calculations using a plane-wave basis set, Phys. Rev. B **54**, 11169 (1996).

[40] G. Kresse and D. Joubert, From ultrasoft pseudopotentials to the projector augmented-wave method, Phys. Rev. B **59**, 1758 (1999).

[41] J. Klimeš, D. R. Bowler, and A. Michaelides, Chemical accuracy for the van der Waals density functional, J. Phys. Condens. Matter **22**, 022201 (2010).

[42] L. E. Bove, R. Gaal, T. C. Hansen, S. Klotz, U. Ranieri, and M. Rescigno, Melting curve and new phases of hydrogen hydrate in the GPa range: A missing piece of information for planetary modelling, Institut Laue-Langevin (ILL), 10.5291/ILL-DATA.5-24-703 (2023).

[43] S. Klotz, K. Komatsu, H. Kagi, K. Kunc, A. Sano-Furukawa, S. Machida, and T. Hattori, Bulk moduli and equations of state of ice VII and ice VIII, Phys. Rev. B **95**, 174111 (2017).

[44] M. Xu, S. Ye, and Z. Bačić, General selection rule in the inelastic neutron scattering spectroscopy of a diatomic molecule confined inside a near-spherical nanocavity, J. Phys. Chem. Lett. **6**, 3721 (2015).

[45] O. Arnold *et al.*, Mantid—data analysis and visualization package for neutron scattering and μSR experiments, Nucl. Instrum. Methods Phys. Res., Sect. A **764**, 156 (2014).

[46] D. Richard, M. Ferrand, and G. J. Kearley, Analysis and visualisation of neutron-scattering data, J. Neutron Res. **4**, 33 (1996).

[47] X. Zhang, T. Karman, G. C. Groenenboom, and A. van der Avoird, Para-ortho hydrogen conversion: Solving a 90-year old mystery, Nat. Sci. **1**, e10002 (2021).

[48] L. E. Bove, R. Gaal, S. Klotz, M. M. Koza, J. Ollivier, and M. Rescigno, Nematic ordering in hydrogen hydrates at high pressure and low temperature, Institut Laue-Langevin (ILL), 10.5291/ILL-DATA.7-02-215 (2023).

[49] L. E. Bove, L. Andriambariarijaonah, R. Gaal, S. Klotz, M. M. Koza, A. Nicholls, J. Ollivier, and M. Rescigno, Nematic ordering in hydrogen hydrates at high pressure and low temperature, Institut Laue-Langevin (ILL), 10.5291/ILL-DATA.7-03-232 (2023).